

Lamellae at a preferential wall

G. T. Pickett^{a)}

Department of Materials Science and Engineering, University of Pittsburgh, Pittsburgh, Pennsylvania 15261

(Received 6 February 1995; accepted 30 August 1995)

The profile of the interfacial plane of a diblock copolymer layer in its lamellar melt phase when it is brought into contact with a hard, smooth substrate is calculated. The chains are in the strong-stretching limit. Far from the substrate, the planes are perpendicular to the substrate, and they become distorted near it by a small wetting preference for one of the components of the copolymer. The profile of the distortion is calculated in an Alexander model by making an analogy to the steady flow of an incompressible fluid. The contact angle between the two components of the copolymer and the substrate is the same as it would be if the blocks were not joined to make diblock copolymers. The approach to this contact angle is characterized by a singularity which is calculated. For any molecular weight and elasticity asymmetry between the components of the copolymer, the curvature of the interface changes sign contrary to the case of the interface between two simple liquids. For most values of asymmetry, the interface is an exponentially damped oscillation. © 1996 American Institute of Physics. [S0021-9606(95)51445-0]

I. INTRODUCTION

Diblock copolymers have received much theoretical and experimental attention.¹ These molecules are composed of chemically incompatible homopolymers bound together with the architecture $(A)_{N_A}-(B)_{N_B}$, so that there are N_A A chemical units on a chain and N_B units of type B. If the blocks were not irreversibly joined, they would spontaneously phase separate, forming macroscopic domains of pure A and B. Bonding the homopolymer blocks forces a phase separation on length scales on the order of tens of nanometers.^{1,2} Equilibrium structures formed by dense droplets composed of these molecules display different degrees of symmetry. The most symmetric is the one considered here, the lamellar. In the bulk, the interfaces between A and B domains are flat planes with the copolymers stretched normal to the interfaces. When the degree of polymerization becomes sufficiently large, the strongly segregated region is entered, and sharp interfaces between A-rich and B-rich phases appear. In this situation, the incompatibility of the A and B fluids can be described by an interfacial energy, γ .

When the polymer blocks are roughly symmetric in volume fraction and elasticity, the lamellar phase is stable. The lamellar phase is often established near an impenetrable substrate, e.g., the thin films produced in spin casting. The morphology of the lamellae is usually determined by interfacial energies. In general, γ_A and γ_B (the energy per unit area to make an interface between A fluid and the wall, and similarly for B) are not equal, and the substrate wets with the lower surface energy block. When the difference in surface energies is small enough³ the lamellar planes can be oriented perpendicularly to the substrate.

The perpendicular morphology is likely to have important technological significance. The exposed lamellar order can be exploited as a template for the ordering of other structures. Differential affinity of the blocks for gold, say, leads to

the possibility that the lamellar order could be decorated with conductors, and produce devices of novel properties.^{4,5} The differential in wetting forces necessarily distorts the lamellar order in the vicinity of the substrate. Characterizing this distortion is important for understanding and gaining control over the orientation of surface lamellae.

In this paper the shape of the AB interface is calculated when the lamellae are in the perpendicular morphology. A greatly simplifying assumption is the Alexander-deGennes approximation.^{6,7} Here, the A block terminates on a single surface, $z=h_A$, and all of the B blocks terminate on the surface $z=-h_B$, with the AB junction points residing at $z=0$. The A and B blocks normally terminate over the entire range $-h_B < z < h_A$. When these ends are distributed in mechanical equilibrium and space is filled with the chains, the distribution of A ends is sharply peaked near $z=h_A$, and likewise with the B ends near $z=-h_B$.⁸ There are indeed qualitative differences between the end-distributed and end-confined systems. But the chain ends are far from the AB interface in both models, so it is expected that the interface calculated in the Alexander-deGennes approximation will qualitatively reflect that for the end-distributed system.

The interface is distorted near the substrate where the difference in wetting energies acts. The shape of this distorted interface is qualitatively unlike the interface formed between two simple liquids, because the polymer chains are able to transmit forces along their backbones. Simple fluids can transmit forces only through a scalar pressure field. The connectivity of the chains allows an analogy to be drawn between a copolymer system and the steady flow of an incompressible, inviscid fluid. This analogy is pursued and made exact in Sec. II. The interfacial profile itself is determined in Sec. III. In Sec. IV, the free-energy associated with creating this distorted interface is calculated, and it is shown that the interface is stable when the influence of wetting forces is included. In Sec. V, it is shown that the fluid flow formalism developed here agrees with the traditional formulation of this problem in the electrostatics language of

^{a)}Electronic mail: pickett@marie.mse.pitt.edu

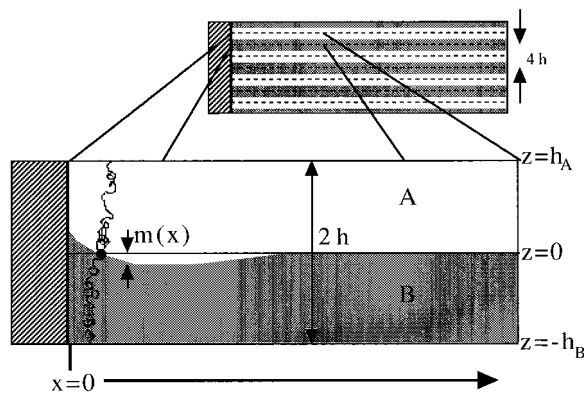


FIG. 1. The lamellae are perpendicular far from the substrate, and are distorted near it by the wetting preference of the wall. The inset is the general morphology, with both components in contact with the wall. The substrate is located at $x=0$. The profile of the interface between A and B is $m(x)$.

Semenov. In Sec. VI, the new features of the interface are explored. Then, in Sec. VII, the stability of the lamellar mid-planes is addressed, and the copolymer system is compared to a system without elasticity (the case of the interface between simple fluids forming a meniscus), and a system in which forces are carried both along the chains and transverse to the chains, i.e., the case of a simple elastic body. When the elastic body is greatly stressed uniaxially, I show that the copolymer case is recovered. My conclusions are set forth in Sec. VIII.

II. FLUID FLOW MODEL

I consider a stack of lamellae in contact with a hard surface at $x=0$, so that the chains run more or less in the \hat{z} direction and the lamellar planes run in the \hat{x} direction. The small quantity ϵ stands for the differential in wetting energy for the A and B fluids to cover the wall, dimensioned by γ .

$$\epsilon = \frac{\gamma_A - \gamma_B}{\gamma}. \quad (1)$$

Let us begin by considering the symmetric case: $\epsilon=0$. Let $z=0$ be the vertical coordinate where the interface intersects the substrate, as in Fig. 1. The Alexander–deGennes approximation is adopted: all of the A chain free ends are held at the plane $z=h_A$, while the B free ends are at $z=-h_B$. The junction of the A and B chains lies on the plane $z=0$. ϵ is now allowed to depart slightly from 0. The junction points migrate away from $z=0$ by an amount $m(x)$, but the surfaces at $z=h_A$ and $z=h_B$ remain flat. These surfaces are reflection symmetry planes of the system. I return to the possibility that this symmetry could break in Sec. VII.

A. The stream function

Let $p(\mathbf{r})$ stand for the free energy per volume to insert a portion of chain at the position \mathbf{r} . For now, p is a fixed field, the hydrostatic pressure (as we see below). The constraints

on p which ensure that the resulting configurations have the correct degree of polymerization and are in mechanical equilibrium will be identified.

The configuration of a single chain is specified by a set of vectors, $\{\mathbf{r}_i\}$, giving the position of the i th chemical repeat unit. Given the chemical structure of the repeating units, finding the set of possible configurations is a formidable problem, even for the simplest polymers. However, for a single polymer chain in a dense liquid of identical chains, $\mathbf{r}_N - \mathbf{r}_0$ has a Gaussian distribution,⁹ so that the ensemble of configurations for a single chain is statistically the same as the paths taken by a random walker. The self-similarity of a random-walker's trajectory justifies breaking a large chain into many identical random walkers taking fewer steps. I think of the A chain as made up of identical units of l_A repeat units so that there are N_A units of length l_A on a chain. I similarly divide the B chain into units of chemical length l_B . I choose l_A and l_B large enough so that the repeat units themselves are statistically random walks. For convenience, I choose l_A and l_B so that the subunits displace the same volume in the melt.

To build up an extended configuration for the copolymer, I need only keep track of the coarse-grained subunits. To maintain the n th repeat unit's ends held at a separation of $\Delta\mathbf{r}$, a free energy must be paid:

$$f_{\text{el}} = \frac{K_A}{2} \Delta\mathbf{r} \cdot \Delta\mathbf{r}, \quad (2)$$

where I define the elastic constant K_A for A-type monomers, and K_B for B-type monomers. From now on, these statistical segments will be referred to as the monomers making up the chain, and they are numbered with the parameter n instead of i .

Let the configuration of a polymer chain in terms of its monomers be $\mathbf{r}(n)$. The free energy associated with this configuration is

$$G[\mathbf{r}(n)] \equiv \int_0^N dn \left(\frac{K}{2} \frac{d\mathbf{r}}{dn} \cdot \frac{d\mathbf{r}}{dn} + p[\mathbf{r}(n)] \right). \quad (3)$$

Given the position $\mathbf{r}(N_A + N_B)$, and the position $\mathbf{r}(0)$, the intermediate chain segments are in mechanical equilibrium when the variation $\delta G / \delta \mathbf{r}(n) = 0$. Thus,

$$K \frac{d}{dn} \frac{d\mathbf{r}}{dn} = \nabla p, \quad (4)$$

equivalent to Newton's law for a particle of mass K in a potential $-p$. It is also identical to Newton's law for fluid particles flowing in the pressure p . The chain extension per monomer, $d\mathbf{r}/dn$, plays the role of the velocity of a tiny amount of fluid, and K plays the role of the mass density of the fluid.

The reduction of the full self-consistent problem to the Alexander–deGennes model is accomplished by observing that the particle velocity is a field in its own right:

$$\frac{d\mathbf{r}}{dn} [\mathbf{r}(n), n] = \mathbf{v}[\mathbf{r}(n)]. \quad (5)$$

The particle motion is *steady*: there is no explicit dependence on monomer number n for the flow pattern. The velocity field is static. Many chains with different velocities coexist at each point in the end-distributed system. It is impossible to define a velocity field which depends only on position in the fully self-consistent model; to specify the velocity of a chain, both the position in space and the monomer number are needed.

In any event, the Alexander–deGennes system is formally identical to the steady flow of a two-dimensional fluid. In particular, let ϕ depend both upon position and monomer number. The change in ϕ from one monomer to the next on the same chain is

$$\begin{aligned} \frac{d\phi}{dn} &= \frac{\partial\phi}{\partial n} + v_x \frac{\partial\phi}{\partial x} + v_z \frac{\partial\phi}{\partial z} \\ &= \frac{\partial\phi}{\partial n} + \mathbf{v} \cdot \nabla\phi, \end{aligned} \quad (6)$$

so that the operator d/dn is given by the usual convective derivative. Thus, Eq. (4) is equivalent to

$$K(\mathbf{v} \cdot \nabla)\mathbf{v} = \nabla p, \quad (7)$$

since $\partial_n \mathbf{v} = 0$. After the application of an elementary identity, this may be written as

$$K\mathbf{v} \times (\nabla \times \mathbf{v}) = \nabla \left(\frac{K}{2} \mathbf{v} \cdot \mathbf{v} - p \right), \quad (8)$$

equivalent to Bernoulli's law.

The systems considered here are composed of dense liquids, and hence are characterized by very small compressibilities. As is customary, the small compressibility of the polymer liquid is neglected, as overall changes in the local density of fluid are of the order of the compressibility of the dense liquid. This assumption is common in the elementary study of fluid dynamics, and it is adopted here. Therefore, each chain is assumed to occupy a fixed volume. The local conservation of particle number leads to the usual equation of continuity; incompressibility thus implies that the velocity field is divergenceless. The two-dimensional (2D) flow mirroring the polymer system must obey

$$\nabla \cdot \mathbf{v} = 0. \quad (9)$$

The bulk behavior of the polymers is governed by Eqs. (7) and (9).

The condition (9) is met when

$$\mathbf{v} = -\partial_z \psi \hat{x} + \partial_x \psi \hat{z} = \nabla \times \mathbf{A}, \quad (10)$$

with the vector potential \mathbf{A} given by,

$$\mathbf{A} = \hat{y} \psi. \quad (11)$$

Here \hat{y} is a unit vector perpendicular to both \hat{x} and \hat{z} , forming a right-handed coordinate system. This choice for \mathbf{A} is traditional for 2D incompressible flows. The function ψ is known as the *stream function*.¹⁰ It is easy to verify that ψ is constant on the streamlines of the flow:

$$\frac{d\psi}{dn} = \mathbf{v} \cdot \nabla \psi = v_x \partial_x \psi + v_z \partial_z \psi = 0. \quad (12)$$

Thus, ψ labels chains.

Equation (8) is now considered in terms of ψ :

$$\nabla^2 \psi \nabla \psi = \nabla \left(\frac{K}{2} \nabla \psi \cdot \nabla \psi - p \right). \quad (13)$$

Taking the curl of both sides of this equation yields an equation determining ψ :

$$\nabla (\nabla^2 \psi) \times \nabla \psi = 0. \quad (14)$$

Curves on which ψ are constant are everywhere parallel to curves on which $\nabla^2 \psi$ are constant. When ψ uniquely specifies the chains, as in the model presented below,

$$\nabla^2 \psi = f(\psi), \quad (15)$$

for some $f(\psi)$, as yet unknown. Since $\nabla \times \mathbf{v} = -\hat{y} \nabla^2 \psi$, $\nabla^2 \psi$, is interpreted to be the vorticity of the flow. Therefore, vorticity is conserved along the streamlines of an incompressible, steady, inviscid flow.¹⁰

Given $f(\psi)$ Eq. (15) must be supplemented by two boundary conditions in order to determine ψ . An additional condition specifies $f(\psi)$, so that a total of three conditions must be given. Or, rather, three conditions must be supplied for each stream function. There are two portions of the copolymer chains, so I break the system into two coupled flows. Thus, Eq. (15) holds for both A and B fluids, with possibly different f_A and f_B .

A further unknown is the interfacial profile, $m(x)$, and a separate condition must be given for it. Therefore a total of seven (3+3+1) conditions must be given to completely specify this system.

B. Boundary conditions

I determine boundary conditions by enforcing Eq. (9) at the AB interface, the mechanical equilibrium of each unconstrained surface, and that each block has the correct number of monomers on it.

Constraint forces normal to the surface at $z = h_A$ maintain $z = h_A$ as the termination surface for A blocks, and similarly at $z = -h_B$ for the B blocks. In the \hat{x} direction, additional forces can arise from the polymer chains arriving at $z = h_A$ with some tangential component to \mathbf{v} . The upper surface cannot support these tangential stresses: the chains rearrange themselves until the tangential stress vanishes near $z = h_A$. In other words,

$$v_x(x, h_A) = 0. \quad (16)$$

Similarly for the B chain ends arriving at the lower surface, $z = -h_B$,

$$v_x(x, -h_B) = 0. \quad (17)$$

In terms of the stream functions ψ_A and ψ_B ,

$$\partial_z \psi_A|_{h_A} = 0, \quad \text{and} \quad \partial_z \psi_B|_{-h_B} = 0. \quad (18)$$

With the two conditions in Eq. (18), the upper and lower surfaces are in mechanical equilibrium.

Now, I turn to the AB interface. An essentially kinematic constraint holds, whose analog hydrodynamically is that the equation of continuity is obeyed at the AB interface. Each B chain which arrives at the interface is joined to a single A chain which leaves the interface. If a^3 is the volume per monomer for both A and B fluids, then $a^{-3}\mathbf{v}\cdot\hat{\mathbf{n}}$ is the number of chains per area crossing the interface, where $\hat{\mathbf{n}}$ is the normal to the interface at $z=m(x)$. Thus, the normal component of \mathbf{v} must be continuous across the interface:

$$\mathbf{v}\cdot\hat{\mathbf{n}}|_{m(x)^+}=\mathbf{v}\cdot\hat{\mathbf{n}}|_{m(x)^-}, \quad (19)$$

or, in terms of ψ_A and ψ_B :

$$\nabla\psi_A\cdot\hat{\mathbf{t}}|_{m(x)}=\nabla\psi_B\cdot\hat{\mathbf{t}}|_{m(x)}, \quad (20)$$

where, $\hat{\mathbf{t}}$ is the *tangential* direction at the interface. This is the third condition.

Two further conditions are needed to ensure the mechanical equilibrium of the AB interface. Forces per unit area arise from three sources: γ at the curved interface acts like an effective pressure (Laplace pressure),¹¹ the differential in pressure across the interface, and the resultant of the chain forces acting on each side of the interface. Therefore, it is noted that

$$F\hat{\mathbf{n}}-\Delta p\hat{\mathbf{n}}+\gamma\frac{d^2m}{dx^2}+\mathbf{v}\cdot\hat{\mathbf{n}}(K_A\mathbf{v}|_{m(x)^+}-K_B\mathbf{v}|_{m(x)^-})=0, \quad (21)$$

where $\Delta p=p|_{m^+}-p|_{m^-}$. This is a vector equation. F is the external driving force. Here, F arises from the difference in wetting energies at the substrate

$$F\hat{\mathbf{n}}=(\gamma_A-\gamma_B)\delta(x)\hat{\mathbf{z}}=\epsilon\gamma\delta(x)\hat{\mathbf{z}}, \quad (22)$$

with ϵ given by Eq. (1). In the tangential direction, Eq. (21) states

$$K_B\mathbf{v}\cdot\hat{\mathbf{t}}|_{m(x)^-}=K_A\mathbf{v}\cdot\hat{\mathbf{t}}|_{m(x)^+}, \quad (23)$$

or, in terms of ψ :

$$K_B\nabla\psi_B\cdot\hat{\mathbf{n}}|_{m(x)}=K_A\nabla\psi_A\cdot\hat{\mathbf{n}}|_{m(x)}. \quad (24)$$

The balance of tangential stress at the AB interface constitutes the fourth constraint needed to specify ψ_A and ψ_B .

In the direction normal to the interface, the balance of forces (21) becomes

$$\epsilon\gamma\delta(x)-\Delta p+\gamma\frac{d^2m}{dx^2}+v_n^2(K_A-K_B)=0, \quad (25)$$

where v_n is the normal component of the velocity at the interface. In terms of ψ , this is

$$\epsilon\gamma\delta(x)-\Delta p+\gamma\frac{d^2m}{dx^2}+(K_A-K_B)[\hat{\mathbf{t}}\cdot\nabla\psi_A]^2|_{m(x)}=0. \quad (26)$$

The condition that the normal forces per unit area on the AB interface are in equilibrium is the fifth condition.

The last two constraints ensure that the chains have the correct number of monomers on them. In this case, the

chains are monodisperse in molecular weight: each has N_A+N_B monomers. That is, the transit time for particles in this flow is constant, with a fixed portion of the time spent above and below the interface. This is the novel component of the problem, for rarely in an elementary fluid problem is one asked to worry about the transit time from one surface to another.

The monomers (or the transit time) are counted as

$$N_A=\int_{[x,m(x)]}^{[x_f,h_A]}dz\frac{1}{v_z[x_c(z),z]}, \quad (27)$$

and,

$$N_B=\int_{[x_i,-h_B]}^{[x,m(x)]}dz\frac{1}{v_z[x_c(z),z]}, \quad (28)$$

where the integration is along a single-chain trajectory, $x_c(z)$ which has initial position $(x_i,-h_B)$, and final position (x_f,h_A) . These are, strictly speaking, integral constraints and not boundary conditions which must be obeyed.

C. Perturbation theory

All dependent variables are expressed in the form

$$\phi=\phi^{(0)}+\epsilon\phi^{(1)}+\dots \quad (29)$$

With $\epsilon=0$, the flow is uniform for both A and B chains:

$$\psi_A^{(0)}=v_0x \quad \text{and} \quad \psi_B^{(0)}=v_0x, \quad (30)$$

by Eqs. (18) and (20). Monodispersity evidently requires that

$$\int_{-h_B}^{h_A}dz\partial_x\psi=(N_A+N_B)\rightarrow v_0=\frac{h_A+h_B}{N_A+N_B}. \quad (31)$$

Also, Eq. (21) implies that

$$p^{(0)}=\begin{cases} K_A v_0^2 & \text{for } z>0 \\ K_B v_0^2 & \text{for } z<0. \end{cases} \quad (32)$$

In addition, the total force in the \hat{x} direction acting on the substrate must vanish:

$$\gamma-K_A v_0^2 h_A-K_B v_0^2 h_B=0. \quad (33)$$

Thus, γ is determined, given h_A , h_B , N_A , and N_B .

Here Eq. (30) is substituted into Eq. (15) and the unknown function f is expanded

$$\nabla^2\psi^{(0)}=f^{(0)}(\psi^{(0)}), \quad (34)$$

or,

$$f^{(0)}(x)=0. \quad (35)$$

This choice of $f^{(0)}$ and $\psi^{(0)}$ evidently satisfies all of the boundary conditions put forth above.

Now, consider Eq. (15) when terms up to the first in ϵ are retained:

$$\nabla^2\psi_A^{(1)}=f_A^{(1)}(\psi_A^{(0)})\equiv\frac{1}{Kv_0}\frac{dg_A^{(1)}(x)}{dx}, \quad (36)$$

where f_A has been replaced with another arbitrary (for now) function g_A . Differentiating this equation with respect to z yields the equation determining $\psi_A^{(1)}$:

$$\partial_z \nabla^2 \psi_A^{(1)} = 0. \quad (37)$$

A similar equation exists for $\psi_B^{(1)}$. In terms of $\mathbf{v}^{(1)}$:

$$\nabla^2 v_x^{(1)} = 0, \quad (38)$$

a familiar result from both Fredrickson *et al.*¹² and Turner and Joanny.¹³ Since $\psi_A^{(1)}$ obeys a third-order differential equation, three conditions must be given to specify it. Also, three conditions must be given to specify $\psi_B^{(1)}$. Along with the determination of a single undetermined surface $m(x)$, this gives a total of seven (3+3+1) conditions to be given for a total specification of this problem in the first order.

The undetermined functions $g_A^{(1)}$ and $g_B^{(1)}$ are related to the pressure p through the analysis of Eq. (7):

$$Kv_0 \partial_z \mathbf{v}^{(1)} = \nabla p^{(1)}. \quad (39)$$

The x component of this equation reads as

$$-Kv_0 \partial_{z,z} \psi^{(1)} = \partial_x p^{(1)}, \quad (40)$$

or, equivalently,

$$Kv_0 \nabla^2 \psi^{(1)} = \partial_x (Kv_0 \partial_x \psi^{(1)} - p^{(1)}). \quad (41)$$

Thus,

$$g^{(1)}(x) = Kv_0 \partial_x \psi^{(1)} - p^{(1)}. \quad (42)$$

Here, the subscripts A for $z > 0$ and B for $z < 0$ have been suppressed. Given $\psi^{(1)}$ and $g^{(1)}$, the pressure is determined.

Boundary conditions in this order are easily handled. The conditions (18) become in the first order:

$$\partial_z \psi_A^{(1)}|_{h_A} = 0, \quad (43)$$

and,

$$\partial_z \psi_B^{(1)}|_{-h_B} = 0. \quad (44)$$

The kinematic condition, (20), is also easy to formulate:

$$\partial_x \psi_A^{(1)}|_0 = \partial_x \psi_B^{(1)}|_0. \quad (45)$$

Similarly, Eq. (24) becomes

$$K_A \partial_z \psi_A^{(1)}|_0 = K_B \partial_z \psi_B^{(1)}|_0. \quad (46)$$

Now, Eq. (27) at first order takes the form

$$v_0 m^{(1)}(x) + \int_0^{h_A} dz \partial_x \psi_A^{(1)} = 0. \quad (47)$$

Differentiating this equation with respect to x , and using Eq. (36) implies that

$$K_A v_0^2 \frac{dm^{(1)}}{dx} + \frac{g_A^{(1)}}{dx} h_A - K_A v_0 \partial_z \psi_A^{(1)} \Big|_0^{h_A} = 0. \quad (48)$$

By an independent boundary condition on $\psi_A^{(1)}$, Eq. (43), this can be written in its final form as

$$K_A v_0^2 \frac{dm^{(1)}}{dx} + \frac{g_A^{(1)}}{dx} h_A + K_A v_0 \partial_z \psi_A^{(1)} \Big|_0 = 0. \quad (49)$$

In exactly the same manner, the following boundary condition ensures that in the first order there are N_B monomers per chain:

$$K_B v_0^2 \frac{dm^{(1)}}{dx} - \frac{g_B^{(1)}}{dx} h_B + K_B v_0 \partial_z \psi_B^{(1)} \Big|_0 = 0. \quad (50)$$

These—Eqs. (49) and (50)—are two further conditions. The final condition enforces the mechanical equilibrium of the interfacial plane in the z direction, to this order.

The pressure p is given by

$$p^{(1)} = \begin{cases} K_A v_0 \partial_x \psi_A^{(1)} - g_A^{(1)}, & \text{when } z > 0 \\ K_B v_0 \partial_x \psi_B^{(1)} - g_B^{(1)}, & \text{when } z < 0. \end{cases} \quad (51)$$

Therefore, the pressure difference across the interface is

$$\Delta p^{(1)} = (K_A - K_B) v_0 \partial_x \psi_A^{(1)}|_0 + g_B^{(1)} - g_A^{(1)}. \quad (52)$$

Thus, the equation for balance of forces at the interface in the z direction amounts to

$$g_B^{(1)}(x) - g_A^{(1)}(x) + (K_B - K_A) v_0 \partial_x \psi_A^{(1)}|_0 - \gamma \frac{d^2 m^{(1)}}{dx^2} = \gamma \delta(x). \quad (53)$$

This is the final condition, given in the form of a boundary condition, for a total of seven: Eqs. (43)–(46), (49), (50), and (53).

Each of these equations can be derived from considering the free energy of the entire layer, i.e., the free energy per unit volume instead of the free energy per chain. The results of each analysis agree in determining the profile $m^{(1)}(x)$, as in sec. V.

III. INTERFACIAL PROFILE

The problem can be solved by using an analog computer. Given a long narrow channel, of length L and width W , a porous membrane is stretched along the width of L spaced Wh_A/h_B from one of the long sides. The membrane has a surface tension γ , and it should allow fluid to flow past it without disturbing it too much. On one of the long sides of the channel, a line of water jets is placed, and sinks are arranged along the other side. To simulate the change of elastic constants across the interface, the density of the liquid changes as it crosses the membrane, say by dissolving salt deposits across the length. The author grabs hold of the membrane where it encounters one of the short walls, and pulls it in the \hat{z} direction. The strength of the sources and the sinks are then adjusted to ensure that the travel time from one surface to the next is constant and that the tangential velocity of the fluid vanishes at both surfaces. When that condition is met, the net force of the fluid on the membrane will cause the membrane to distort into the profile this calculation predicts.

So, what profile does this model predict? The most general solution to Eq. (36) which obeys Eqs. (43) and (44) is

$$\psi_A^{(1)}(x,z) = \int_{-\infty}^{\infty} \frac{dq}{2\pi} \frac{1}{iq} e^{iqx} \left(C_A(q) \cosh(qz - qh_A) + \left(\frac{K_B}{K_A} - 1 \right) g_A^{(1)}(q) + \gamma q^2 m(q) = 2\gamma. \right. \\ \left. + \frac{g_A^{(1)}(q)}{K_A v_0} \right), \quad (54)$$

and equivalently for $\psi_B^{(1)}$:

$$\psi_B^{(1)}(x,z) = \int_{-\infty}^{\infty} \frac{dq}{2\pi} \frac{1}{iq} e^{iqx} \left(C_B(q) \cosh(qz + qh_B) + \frac{g_B^{(1)}(q)}{K_B v_0} \right). \quad (55)$$

Five conditions must be met to determine all of the unknowns.

The Fourier transform for ψ are used. As a mathematical convenience, the *even* continuation of $\psi_A^{(1)}$, $\psi_B^{(1)}$, and $m^{(1)}(x)$ are chosen. The situation is equivalent to placing two copolymer domains back to back, and subjecting them both to the wetting force. Therefore, the magnitude of the wetting force must double. The constraint imposed by the wall is that $v_x(0,z)=0$, and this is obeyed by the even continuation. The fact that a hard wall can be replaced by an appropriate symmetry is well known.¹⁴

The pressure $p^{(1)}$ is given by

$$p^{(1)}(x,z) = \int_{-\infty}^{\infty} \frac{dq}{2\pi} e^{iqx} K_A v_0 C_A(q) \cosh(qz - qh_A) \\ \text{when } z > 0, \quad (56)$$

and

$$p^{(1)}(x,z) = \int_{-\infty}^{\infty} \frac{dq}{2\pi} e^{iqx} K_B v_0 C_B(q) \cosh(qz + qh_B) \\ \text{when } z < 0. \quad (57)$$

The conditions (45), (46), (49), (50), and (53) thus reduce to algebraic equations among the five remaining unknown quantities: $C_A(q)$, $C_B(q)$, $g_A^{(1)}(q)$, $g_B^{(1)}(q)$, and $m^{(1)}(q)$:

$$C_A(q) \cosh(qh_A) + \frac{g_A^{(1)}(q)}{K_A v_0} \\ = C_B(q) \cosh(qh_B) + \frac{g_B^{(1)}(q)}{K_B v_0}, \quad (58)$$

$$-K_A C_A(q) \sinh(qh_A) = K_B C_B(q) \sinh(qh_B), \quad (59)$$

$$K_A v_0^2 q m^{(1)}(q) + q h_A g_A^{(1)}(q) + K_A v_0 C_A(q) \sinh(qh_A) = 0, \quad (60)$$

$$K_B v_0^2 q m^{(1)}(q) - q h_B g_B^{(1)}(q) - K_B v_0 C_B(q) \sinh(qh_B) = 0, \quad (61)$$

and

$$g_B^{(1)}(q) - g_A^{(1)}(q) + (K_B - K_A) v_0 C_A(q) \cosh(qh_A)$$

The problem is reduced to solving this set of five equations in five unknowns, conceptually trivial but complicated to work out by hand.

For the moment, consider the system of four equations, (58)–(61). This set of equations ensures that the polymer trajectories are monodisperse, that they intersect the surfaces $z=h_A$ and $z=-h_B$ at normal incidence, that the tangential thrust across the interface is continuous, as well as the kinematic condition that the normal velocity at the interface is continuous. So, given any first-order interfacial profile $m^{(1)}(x)$ imposed by hand, this set of equations determines the distortion of the polymer trajectories

$$C_A(q) = - \frac{m^{(1)}(q)(h_A + h_B)q^2 K_B v_0}{F_1 + F_2}, \quad (63)$$

where

$$F_1 = (h_A q K_A + h_B q K_B) \sinh h_A q, \quad (64)$$

and

$$F_2 = -h_A h_B q^2 (K_A \sinh h_A q \coth h_B q + K_B \cosh h_B q). \quad (65)$$

Additionally,

$$C_B(q) = -C_A(q) \quad \text{with } K_A \leftrightarrow K_B \text{ and } h_A \leftrightarrow h_B. \quad (66)$$

Similarly ghouly expressions exist for $g_A^{(1)}$ and $g_B^{(1)}$:

$$g_A^{(1)} = m^{(1)}(q) q K_A v_0^2 \frac{F_3}{F_1 + F_2}, \quad (67)$$

where

$$F_3 = (K_B - K_A) \sinh h_A q + h_B q (K_A \sinh h_A q \coth h_B q + K_B \cosh h_B q). \quad (68)$$

Additionally,

$$g_B^{(1)} = -g_A^{(1)} \quad \text{with } K_A \leftrightarrow K_B \text{ and } h_A \leftrightarrow h_B. \quad (69)$$

The last equation to deal with determines $m^{(1)}$.

I define dimensionless parameters: let $2h = h_A + h_B$ be the basic scale of length, and let the volume fraction of B per chain be f so that

$$h_A = 2(1-f)h, \quad \text{and } h_B = 2fh. \quad (70)$$

Let $\bar{K} = (K_A + K_B)/2$, and define a reduced elasticity k_A so that $K_A = k_A \bar{K}$ and $K_B = k_B \bar{K}$. Thus, Eq. (33) implies that

$$\gamma = v_0^2 (2h) \bar{K} [(1-f)k_A + fk_B] \\ = (2h)^3 N^{-2} \bar{K} [(1-f)k_A + fk_B]. \quad (71)$$

With this notation, $k_A + k_B = 2$, so that the only independent parameters are k_A and f , with $0 \leq f \leq 1$ and $0 \leq k_A \leq 2$. For fixed h , f , and k_A , γ is uniquely specified, and given γ , f , and k_A , the lamellar repeat spacing, $4h$, is determined.

The Fourier transform of the midplane interface is thus, using Eqs. (63)–(68) in Eq. (62),

$$\left[\frac{m^{(1)}(q)}{2h^2} \right]^{-1} = q^2 h^2 + \frac{a_1 + a_2 + a_3 + a_4}{2[(1-f)k_A + f(2-k_A)](b_1 + b_2 + b_3)}, \quad (72)$$

with

$$\begin{aligned} a_1 &= 4(1-f)qh(2-k_A)^2 \cosh [2(1-f)qh] \\ &\quad \times \sinh(2fqh), \\ a_2 &= 4fqhk_A^2 \cosh(2fqh) \sinh [2(1-f)qh], \\ a_3 &= -8(k_A-1)^2 \sinh [2(1-f)qh] \sinh(2fqh), \\ a_4 &= 2(1-2f)k_A(2-k_A)qh \sinh [2(1-2f)qh], \\ b_1 &= 4f(1-f)(2-k_A)qh \cosh [2(1-f)qh] \\ &\quad \times \sinh(2fqh), \\ b_2 &= 4f(1-f)k_Aqh \cosh(2fqh) \sinh [2(1-f)qh], \\ b_3 &= [-2(1-f)k_A + f(2-k_A)] \sinh [2(1-f)qh] \\ &\quad \times \sinh(2fqh). \end{aligned} \quad (73)$$

For small qh ,

$$\begin{aligned} m^{(1)}(q) &= \frac{32 f^2 (1-f)^2 [4f(1-f)(1-k_A)^2 + k_A(2-k_A)]}{3k_A(2-k_A)} \\ &\quad \times q^2 h^4 + O[q^4 h^6], \end{aligned} \quad (74)$$

and for $qh \rightarrow \infty$,

$$m^{(1)}(q) = 2q^{-2} + h^2 O[(qh)^{-4}]. \quad (75)$$

The simplicity of Eq. (75) is explored in Sec. VI.

IV. FREE ENERGY, G , AT SECOND ORDER

The free energy gained by the distorted layer is calculated by letting ϵ grow from 0 to ϵ_f , keeping track of the work the interface does on the layer,

$$G = -m(x=0)\epsilon_f \gamma + \int_0^{m(x=0)} dy \epsilon \gamma. \quad (76)$$

At second order, this becomes,

$$G^{(2)} = -m(x=0)\epsilon_f \gamma + m^{(1)} \gamma \int_0^{\epsilon_f} d\epsilon \epsilon, \quad (77)$$

or

$$G^{(2)} = -\frac{\epsilon_f^2}{2} \gamma m^{(1)}(x=0). \quad (78)$$

If $G^{(2)}$ were positive, then the lamella would do work on the substrate, and the interfacial plane would spontaneously distort for $\epsilon=0$. Figure 2 shows $m^{(1)}(x=0)$ for the entire allowed range of $0 < f < 1$ and $0 < k_A < 2$. The author notes that $m^{(1)}(x=0)$ is discontinuous at $k_A=0$. As we shall see, this is characteristic of the interface formed between simple fluids.

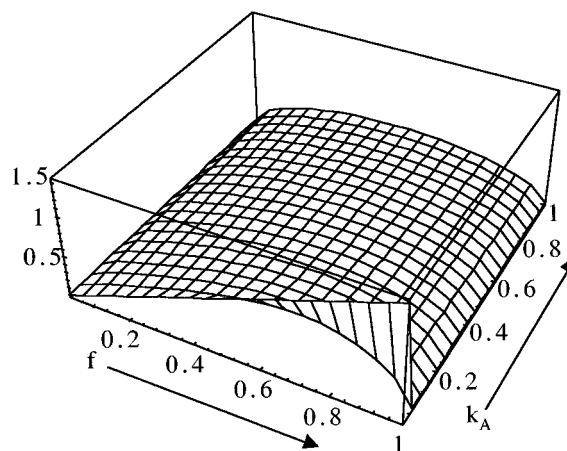


FIG. 2. $m^{(1)}(x=0)h^{-1}$ obtained numerically is plotted for $0 < f < 1$ and $0 < k_A < 1$. To determine $m^{(1)}(x=0)$ when $1 < k_A < 2$, let $f \rightarrow 1-f$. Note the improper limit, $k_A \rightarrow 0$.

The author concludes that, provided the midplane interfaces at $z=h_A$ and $z=-h_B$ are held flat, the interface calculated here is stable.

V. ELECTROSTATIC FORMALISM OF SEMENOV

The quadratic form for the elastic energy density, and the divergencelessness of the velocity field have prompted the framing of this type of system in a formalism resembling electrostatics,¹⁵ which is refined in Refs. 12 and 13. The basic strategy for these calculations is to write a free energy functional for the configuration of the polymer chains, include the various constraints through the use of Lagrange multiplier potentials, and then appropriately minimize the free energy. This program, is followed here and it is demonstrated that the fluid-flow formalism of Sec. II is equivalent to the Semenov's formalism, as well as computationally more concise.

The formulation can be simplified somewhat by writing that

$$v_x(x,z) = -\partial_z \psi, \quad \text{and} \quad v_z(x,z) = \partial_x \psi, \quad (79)$$

where the stream function, ψ , is, as yet, an arbitrary differentiable function. Writing \mathbf{v} thus is a direct consequence of $\nabla \cdot \mathbf{v} = 0$, as above. Thus, incompressibility need not be handled as a separate constraint, and the potential " ϕ " in Ref. 12 need not be included. The potential ϕ has a natural interpretation in Semenov's formalism as the electrostatic potential, whose role is to maintain the divergencelessness of the field configuration. As the velocity field is hypothesized to arise from a vector potential, this constraint is met.

The set of coordinates defined above are used, so that the A polymers are in the region $m(x) < z < h_A$, and B polymers are in the region $-h_B < z < m(x)$. The elastic energy density for A polymers, f_{el} , is given by

$$f_{el} = \frac{K_A}{2} \mathbf{v} \cdot \mathbf{v} = \frac{K_A}{2} (\partial_z \psi_A^2 + \partial_x \psi_A^2) = \frac{K_A}{2} \nabla \psi_A \cdot \nabla \psi_A. \quad (80)$$

Note that there are two stream functions needed for the two blocks of the copolymer.

The free energy of the lamella is

$$G[\psi_A, \psi_B, m, \tilde{g}_A, \tilde{g}_B] = \int_0^\infty dx \int_{m(x)}^{h_A} dz \frac{K_A}{2} \nabla \psi_A \cdot \nabla \psi_A + \int_{-h_B}^{m(x)} dz \frac{K_B}{2} \nabla \psi_B \cdot \nabla \psi_B + \tilde{g}_A(x_m) \left(\int_{m(x_m)}^{h_A} \frac{dz}{\partial_x \psi_A(x_c, z)} - N_A \right) + \tilde{g}_B(x_m) \left(\int_{-h_B}^{m(x_m)} \frac{dz}{\partial_x \psi_B(x_c, z)} - N_B \right) + \gamma \sqrt{1 + \frac{dm^2}{dx}} - \epsilon \gamma \delta(x) m(x). \quad (81)$$

The potentials \tilde{g}_A and \tilde{g}_B are related to g_A and g_B above. They enforce monodispersity along each chain, according to the prescription of Refs. 12 and 13. The quantity $x_c(z)$ gives the lateral position, along the chain contour, at the height z , and x_m is the lateral position at which the chain crosses the AB interface. Already, the relative simplicity of the fluid analogy is evident.

In order to determine the equilibrium configuration for ψ and $m(x)$, G is varied with respect to each of its arguments and then boundary conditions are imposed. The variation of G with respect to ψ is complicated by the fact that x_c is determined by ψ :

$$x_c(z) = \int_{-h_B}^z dz \frac{-\partial_z \psi_B(x_c, z)}{\partial_x \psi_A(x_c, z)}. \quad (82)$$

It is necessary to employ perturbation theory to make progress in this model.

The zeroth-order system has the following physical solution:

$$\psi_A^{(0)}(x, z) = v_0 x = \frac{2h}{N} x, \quad (83)$$

$$m(x)^{(0)} = 0, \quad (84)$$

$$x_c^{(0)} = x, \quad (85)$$

$$\gamma = (K_A h_A + k_B h_B) v_0^2, \quad (86)$$

and, along with Refs. 12 and 13, let $\tilde{g}_A^{(0)} = 0$, $\tilde{g}_B^{(0)} = 0$.

The driving term in the free energy is proportional to ϵ [$\epsilon m^{(1)}(x=0)$], so I consider $G^{(2)}$. The task is to write down the full expansion of Eq. (81) to second order:

$$G^{(2)} = \int_0^\infty dx \int_0^{h_A} dz \left(\frac{K_A}{2} \nabla \psi_A^{(1)} \cdot \nabla \psi_A^{(1)} + K_A v_0 \partial_x \psi_A^{(2)} \right) + \int_{-h_B}^0 dz \left(\frac{K_B}{2} \nabla \psi_B^{(1)} \cdot \nabla \psi_B^{(1)} + K_B v_0 \partial_x \psi_B^{(2)} \right) - K_A m^{(1)}(x) \times v_0 \partial_x \psi_A^{(1)} \Big|_0 + K_B m^{(1)}(x) v_0 \partial_x \psi_B^{(1)} \Big|_0 + (K_B - K_A) \frac{v_0^2}{2} m^{(2)}(x) + \tilde{g}_A^{(1)} v_0^{-1} \left(-m^{(1)}(x) - \int_0^{h_A} dz + \frac{\partial_x \psi_A^{(1)}}{v_0} \right) + \tilde{g}_B^{(1)} v_0^{-1} \left(m^{(1)}(x) - \int_{-h_B}^0 dz \frac{\partial_x \psi_B^{(1)}}{v_0} \right) + \frac{\gamma}{2} \left| \frac{dm^{(1)}}{dx} \right|^2 - \epsilon^2 \gamma \delta(x) m^{(1)}(x). \quad (87)$$

There are contributions in $G^{(2)}$ which arise from higher orders in perturbation theory, e.g., $m^{(2)}$. These intrinsically second-order quantities cannot affect the equations of motion for any first-order quantities, so the author proceeds with the standard Euler-Lagrange minimization. It is found that

$$\frac{\delta G^{(2)}}{\delta \psi_A^{(1)}} = 0 \rightarrow K_A \nabla^2 \psi_A^{(1)} - v_0^{-2} \frac{\tilde{g}_A^{(1)}}{dx} = 0, \quad (88)$$

$$\frac{\delta G^{(2)}}{\delta \psi_B^{(1)}} = 0 \rightarrow K_B \nabla^2 \psi_B^{(1)} - v_0^{-2} \frac{\tilde{g}_B^{(1)}}{dx} = 0, \quad (89)$$

$$\frac{\delta G^{(2)}}{\delta m^{(1)}} = 0 \rightarrow v_0^{-1} \tilde{g}_B^{(1)} - v_0^{-1} \tilde{g}_A^{(1)} + (K_B - K_A) v_0 \partial_x \psi_A^{(1)} \Big|_0 - \gamma \frac{d^2 m^{(1)}}{dx^2} = \gamma \delta(x). \quad (90)$$

The author has used Eq. (20) to simplify the results. The following identifications are made:

$$g_A^{(1)}(x) = \tilde{g}_A^{(1)} v_0^{-1}, \quad (91)$$

$$g_B^{(1)}(x) = \tilde{g}_B^{(1)} v_0^{-1}, \quad (92)$$

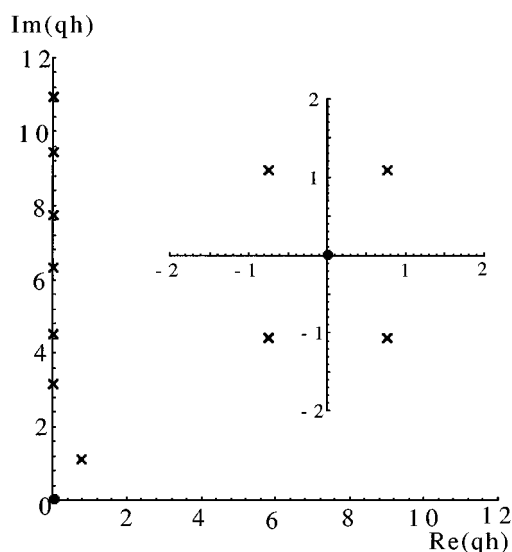


FIG. 3. The analytic structure of $m^{(1)}(q)$ is presented. The second-order zero at the origin ensures incompressibility, and a series of simple poles along the imaginary axis are responsible for the nonanalytic correction to Young's law. The off-axis poles give $m^{(1)}(x)$ its characteristic oscillation.

so that Eqs. (36) and (53) are reproduced. With the further imposition of normal chain incidence at h_A and $-h_B$ and continuity at the interface, Semenov's formalism is identical to the hydrodynamic formalism above.

VI. RESULTS

A. General f and k_A

Figure 3 shows the analytic structure of $m^{(1)}(q)$ schematically. According to Eq. (74), $\lim_{q \rightarrow 0} m^{(1)}(q) = 0$ for all f and $k_A \neq 0, 2$. Therefore,

$$\int_0^\infty \frac{dx}{2\pi} m^{(1)}(x) = m^{(1)}(q=0) = 0. \quad (93)$$

Thus, the incompressibility of the system is confirmed. Each A chain which encounters the interface brings along with it a B chain of fixed volume; thus there can be no excess of A over B. The possible exception is when $k_A = 0$ or 2. Then, one of the blocks is completely flexible. There is no penalty to rearrange the flexible blocks, and extra monomers can be imported from far positions.

Evidently, as $|q| \rightarrow \infty$, there is an essential singularity in $m^{(1)}(q)$. According to Eq. (75), as q becomes large through real values, $m^{(1)}(q) \approx 2q^{-2} + O[(qh)^{-4}]h^2$. This fact determines $\lim_{x \rightarrow 0} dm^{(1)}/dx$. Let $q_m \gg h^{-1}$ be such that when $q > q_m$, $m^{(1)}(q)$ can be replaced with $2q^{-2}$ with negligible error. Let $x \ll h$ be such that $xq_m \ll 1$ as well. Then,

$$\begin{aligned} \frac{dm^{(1)}}{dx} &= - \int_0^{q_m} \frac{dq}{\pi} q \sin(qx) m^{(1)}(q) \\ &\quad - \int_{q_m}^\infty \frac{dq}{\pi} \sin(qx) 2q^{-1}. \end{aligned} \quad (94)$$

The first term above vanishes as $x \rightarrow 0$. The second term has a finite limit as $x \rightarrow 0$:

$$\frac{dm^{(1)}}{dx} = - \int_0^\infty \frac{dy}{\pi} 2y^{-1} \sin y + O[x] = -1 + O[x]. \quad (95)$$

where the variables have been changed in the integral to $y = qx$. Thus, Young's law of wetting is recovered. When a droplet of material A in a medium of fluid B adheres to a substrate, it encounters the substrate with a characteristic angle θ . According to Young's law¹⁶ (which amounts to simply resolving the surface tensions at the interface):

$$\cos \theta = \frac{\gamma_B - \gamma_A}{\gamma} = -\epsilon. \quad (96)$$

In the copolymer problem,

$$\cos \theta = - \frac{\epsilon dm^{(1)}/dx}{\sqrt{1 + [\epsilon dm^{(1)}/dx]^2}} \Big|_{x=0} = -\epsilon + O[\epsilon^2]. \quad (97)$$

Thus, the *wetting angle* between the copolymer blocks and the substrate is in accordance with Young's law. Near the contact line, the interfacial energy dominates the elastic energy.

The function $m^{(1)}(q)$ has a number of simple poles. There are four symmetric poles with both real and imaginary parts. Upon inverse Fourier transforming $m^{(1)}(q)$, these poles impart an oscillation to $m^{(1)}(x)$: the interface crosses $z=0$ infinitely many times, a novel property indeed. Even when all of the poles reside on the imaginary axis, incompressibility and $\lim_{x \rightarrow \infty} m^{(1)}(x) = 0$ implies that the interface must cross $z=0$ at least once. For surfactant bilayers, a similar oscillating relaxation is predicted.¹⁷ For small amplitude of disturbance, the simple liquid system and the surfactant system are handled in the Appendix. Figure 4 shows the location of the pole responsible for the oscillation of the interface for the entire range of f and k_A .

The family of poles residing on the imaginary axis determines the details of the interfacial profile. In the various limits below, these poles are analyzed and first corrections to Young's law are calculated.

B. Symmetric copolymers: $f=1/2$, $k_A=1$

When $f=1/2$ and $k_A=1$, the interfacial profile (72) takes the form

$$m^{(1)}(q) = \frac{2h^2}{(qh)^2 + \frac{1}{1 - (qh)^{-1} \tanh(qh)}}. \quad (98)$$

The poles of $m^{(1)}(q)$ are considered here. The poles at $q = \pm 0.7530 \pm i1.0818$ imply a damped oscillation for $m^{(1)}(x)$ at large x . There is also an infinite series of simple poles along the imaginary axis. The poles which exist at high imaginary q determine the short-distance behavior of $m^{(1)}(x)$. These poles occur when $\tanh(qh) \sim qh$, or for

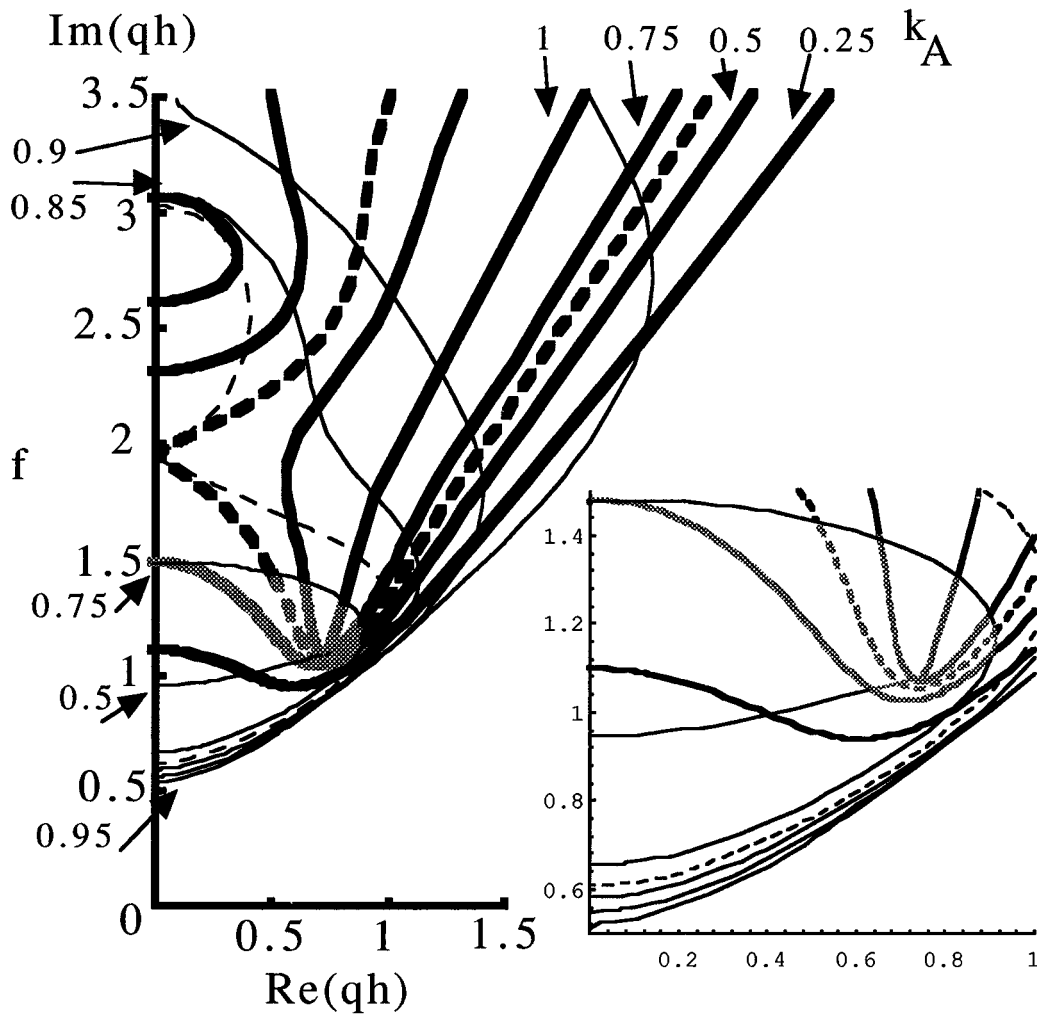


FIG. 4. Here, the position of the pole responsible for the oscillation of the interface is given for arbitrary k_A and f . The thick lines have k_A held constant, and the thin lines have f held constant. The grey portion of the curves indicates the region for which $0.25 < f < 0.75$ and $0.5 < k_A < 1.5$. This most symmetric region for f and k_A always has a pole off the imaginary axis, so that the interface oscillates. The dashed lines have $k_A = 0.6384$ and $f = 0.809$. The inset is a closeup of the symmetric region.

$$q_n \approx (2n + 1) \frac{i\pi}{2} \quad \text{for } 1 \ll n. \tag{99}$$

The residue at a pole of $m^{(1)}$ can easily be found: if q_0 is the location of a pole of $m^{(1)}(x)$, then

$$\text{Res}[m^{(1)}(q)]|_{q_0} = \frac{-2h}{(q_0 h)^5 + 2(q_0 h)^3}, \tag{100}$$

a remarkably simple result, given the complexity of Eq. (98). The structure of $m^{(1)}(x)$ can now be determined for very small x .

$m^{(1)}(q)$ is inverse Fourier transformed as follows:

$$m^{(1)}(x) = \int_{-\infty}^{\infty} \frac{dq}{2\pi} e^{iqx} \times \frac{2h^2}{(qh)^2 + \frac{1}{1 - (qh)^{-1} \tanh(qh)}}. \tag{101}$$

For $x > 0$, the author closes the contour in this integral with $\text{Im } q > 0$ and enumerates the poles of $m^{(1)}(q)$ so that q_0 and q_1 are the off-axis poles in the first and second quadrants. The remaining poles with $\text{Im}(q) > 0$ are numbered successively as the author goes up the imaginary axis. Then,

$$m^{(1)}(x) = - \sum_{n=0}^{\infty} 4h\pi i \frac{e^{iq_n x}}{(q_n h)^5 + 2(q_n h)^3}. \tag{102}$$

This series is then broken up into two parts, with M being such that $n > M$ causes the $(q_n h)^3$ term to be negligible. Then,

$$m^{(1)}(x) \approx f(x) + 4h \sum_{n=M}^{\infty} \exp\left(-\frac{(2n+1)\pi x}{2h}\right) \times \left(\frac{(2n+1)\pi}{2h}\right)^{-5}, \tag{103}$$

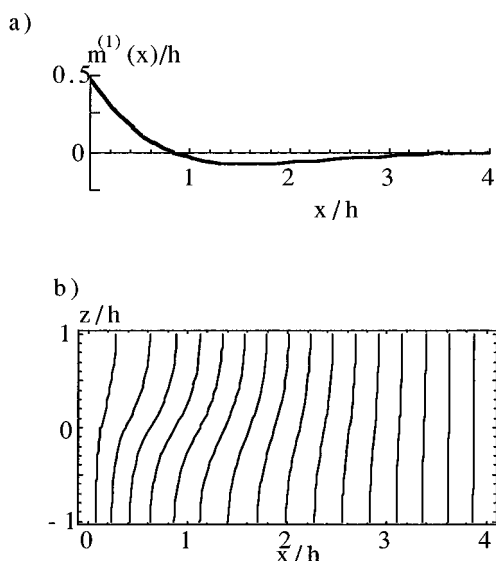


FIG. 5. (a) The shape of the interfacial profile, $m^{(1)}(x)$, scaled by h for symmetric copolymers. (b) These are the streamlines for symmetric copolymers when $\epsilon=1/3$. The chains are everywhere parallel to the lines drawn. The streamlines shown separate equal numbers of chains.

where $f(x)$ is an analytic function of x . The second term in this expression leads to interesting nonanalytic behavior for $m^{(1)}(x)$ near $x=0$. Let $m_{\text{sing}}(x)$ stand for this series: consider,

$$\frac{d^5}{dx^5} m_{\text{sing}}(x) = -4h \sum_{n=N}^{\infty} \exp\left(-\frac{(2n+1)\pi x}{2h}\right) \sim \frac{1}{x}. \quad (104)$$

The fifth derivative of $m_{\text{sing}}(x)$ is singular. Thus, there are nonanalytic corrections to Young's law:

$$m^{(1)}(x) = m^{(1)}(0) - x + (\text{analytic}) + ch^{-3}x^4 \log x/h. \quad (105)$$

The presence of this singularity should be extremely difficult to detect.

Figure 5(a) shows the configuration of the interface, $m^{(1)}(x)$ for symmetric copolymers, and Fig. 5(b) shows the configuration of the polymer chains when $\epsilon=1/3$.

C. Molecular weight asymmetry: $f \neq 1/2$, $k_A = 1$

When the copolymers are made of species of similar elasticity, but of differing molecular weights, the Fourier transform of the interfacial profile (72) becomes

$$m^{(1)}(q) = \frac{2}{(qh)^2 + c/d}, \quad (106)$$

with

$$c = (qh) \sinh(2qh), \quad (107)$$

$$d = 4f(1-f)qh \sinh(2qh) - 2 \sinh(2fqh) \sinh[2(1-f)qh]. \quad (108)$$

This case shares many of the properties of the totally symmetric case, but there is a competition between two length scales, h and $2fh$, and this complicates the analysis.

If a pole of $m^{(1)}$ is located at $qh = y_0$, then y_0 satisfies the following:

$$y_0^{-1} + 4f(1-f)y_0 = \frac{2 \sinh(2fy_0) \sinh[2(1-f)y_0]}{\sinh 2y_0}, \quad (109)$$

and the residue at y_0 is given by

$$\text{Res}[m^{(1)}(q)]|_{(q=y_0/h)} = \frac{h\{y_0 + y_0[2f(1-f)y_0^2 + 2^{-1}]\}}{H(2fy_0) + H[2(1-f)y_0] - H(2y_0) - 1}, \quad (110)$$

where

$$H(x) = x \coth x. \quad (111)$$

When f takes a generic real value, and $|y_0|$ is large, then Eq. (109) is satisfied when $\sinh(2y_0)$ is small:

$$\sinh(2y_0) \sim \frac{\sinh(2fy_0) \sinh[2(1-f)y_0]}{2f(1-f)y_0}. \quad (112)$$

With this condition, the residue at y_0 is approximately

$$\text{Res}[m^{(1)}]|_{q=y_0/h} \approx hf^{-2}(1-f)^{-2}y_0^{-5} \times \sinh^2(2fy_0)/4. \quad (113)$$

For a pole with large and imaginary y_0 , the absolute value of the residue is strictly bounded by hy_0^{-5} , so that the nonanalyticity is at least no worse than in the symmetric case. For generic values of f (i.e., $\sin 2y = \sin 2fy = 0$ should have only $y=0$ as a solution), the author lets $\sinh^2(2fy_0) \rightarrow 1/2$, so that

$$m^{(1)}(x) = \text{analytic} + c'(f)x^4h^{-3} \log(x/h). \quad (114)$$

Allowing asymmetric f does not qualitatively change the correction to Young's law.

For $f \ll 1/2$, Eq. (109) becomes

$$y_0^{-2} + f^2 4(-1 + 2y_0 \coth 2y_0) = 0. \quad (115)$$

If $y_0 = x_0 + iz_0$, then it is deduced that

$$z_0/x_0 \approx \sqrt{3}, \quad \text{and} \quad |y_0| \approx 1/2 f^{-2/3}. \quad (116)$$

When the copolymers become very asymmetric in molecular weight, the range of the ripples is drastically cut.

D. Elastic constant asymmetry: $f=1/2$, $k_A \neq 1$

When the copolymers are symmetric in molecular weight, but are composed of two species of differing elasticities, the interfacial profile takes a relatively simple form. With $f=0.5$ in Eq. (72),

$$m^{(1)}(q) = \frac{2}{(qh)^2 + \frac{1}{2} \frac{k_1 - k_2 \tanh(qh)/(qh)}{1 - \tanh(qh)/(qh)}}, \quad (117)$$

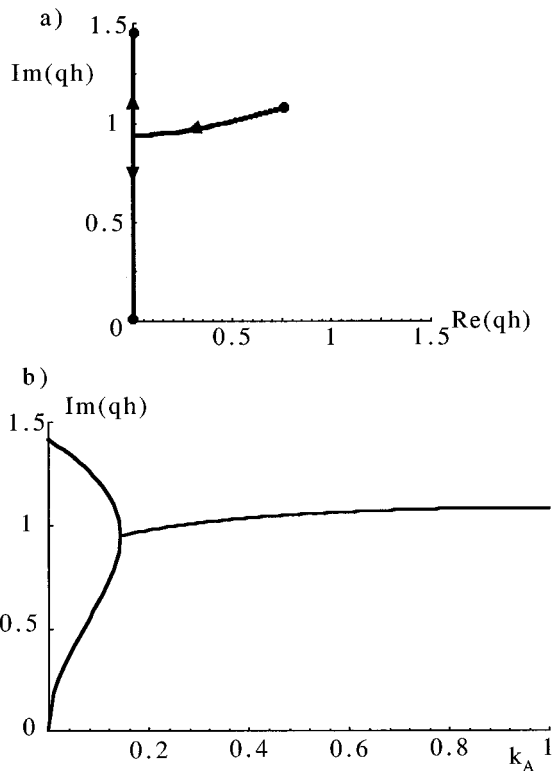


FIG. 6. (a) The position of the off-axis pole is plotted for the range of $0 < k_A < 1$, when $f = 1/2$. (b) The imaginary part of the off-axis pole is plotted against k_A .

where

$$k_1 = 2k_A^2 - 4k_A + 4, \quad (118)$$

$$k_2 = 4(k_A - 1)^2. \quad (119)$$

Figure 6 shows the position of the pole located in the first quadrant as k_A is tuned from 1 to 0 (since the problem has the symmetry $k_A \rightarrow 2 - k_A$). The pole's position starts out with a large real part, which diminishes as the polymer becomes more and more asymmetric. When $k_A = 0.143$, the poles from the first and second quadrants join and then stick to the imaginary axis. The interfacial profile in real space cannot oscillate, but it overshoots $z = 0$ just the same. The oscillation of the interface changes from underdamped to overdamped at $k_A = 0.143$. For smaller k_A , one pole migrates toward the origin, where it destroys the second-order zero. The other one migrates toward $q = \sqrt{2}/h$. This situation recalls that found in the Appendix, where the interface between a liquid drop characterized by both a surface tension and a bending energy forms a meniscus near a vertical wall.

The nonanalytic correction to Young's law still holds for any $k_A \neq 0, 2$. The poles residing on the imaginary axis occur for large q when $\tanh(q) \approx q$, i.e., when $q = (n + 1/2)i\pi$ for large n . It is easy to demonstrate that the residue at a pole, q_0 , of $m^{(1)}(q)$ is given by

$$\text{Res}[m(q)]|_{q_0} = \frac{-2h}{r_{-1}(q_0h)^{-1} + r_1(q_0h) + r_3(q_0h)^3 + r_5(q_0h)^5}, \quad (120)$$

where

$$r_{-1} = 2(k_A - 1)^2, \quad (121)$$

$$r_1 = \frac{(k_A - 1)^2(k_A^2 - 2k_A + 4)}{k_A(2 - k_A)}, \quad (122)$$

$$r_3 = 2 \frac{k_A^2 - 2k_A + 2}{k_A(2 - k_A)}, \quad (123)$$

$$r_5 = \frac{1}{k_A(2 - k_A)}. \quad (124)$$

The residue at a pole located with large iq asymptotically scales as $(qh)^{-5}$, so

$$m^{(1)}(x) = \text{analytic} + c'' k_A(2 - k_A)x^4 \log(x/h). \quad (125)$$

When one of the species is completely flexible, the nonanalytic correction to Young's law vanishes.

When $k_A = 0$, the interfacial profile (72) becomes (for any f)

$$m^{(1)}(q) = 2 \frac{(2fh)^2}{(2fhq)^2 + 2}, \quad (126)$$

so

$$m^{(1)}(x) = \sqrt{2} f h e^{-x/(\sqrt{2}fh)}. \quad (127)$$

The interface is just a single exponential, with length scale equal to the width of the stiffer component of the copolymer. The interface does not cross $z = 0$. This is exactly the interface between simple liquids, as in the Appendix.

VII. DISCUSSION

The shape of the interface is always an overdamped or an underdamped oscillation. And, when reasonably symmetric values for k_A and f are used, the interface is always an underdamped oscillation. Only in extreme cases (k_A is very small) can this result break down. The lamellar phase is unlikely to be the equilibrium structure the copolymers adopt under such extreme conditions. When lamellae are stable, and can be made to orient perpendicularly, the shape of the interface is known. It must cross $z = 0$, and probably oscillates.

However, the analysis is based on the assumption that unperturbed lamellae are indeed flat. The question as to whether lamellar domains are prone to a rippling instability is an open one, so that the absolutely flat geometry considered here may not be the equilibrium configuration of even a realistic lamella.¹⁸ In the Alexander-deGennes approximation, bulk lamellae are unstable to the rippling for wave numbers larger than about h^{-1} .¹⁹ The comparison the author wishes to draw in this paper is to lamellar domains in real systems, i.e., with free ends distributed throughout the layer. "Real" lamellae in end-distributed systems show little sign

of a rippling instability, and are quite flat in the bulk on length scales much smaller than h . Therefore, by insisting that the midplanes interfaces are held flat, the author hopes to capture a crucial qualitative feature of the realistic systems available to experiment.

There is always the possibility that the weak singularity calculated as the first correction to Young's law is an artifact of the Alexander–deGennes approximation that is used throughout this paper. This approximation incorporates the main features that give these copolymer domains their shape, but not rigorously. The robust predictions of this model are that Young's law is satisfied near the contact line, that the interface crosses $z=0$ at least once, and that the interface can oscillate. In the Appendix, the author shows that any stiff, elastic membrane can oscillate when the stiffness is large enough.

The striking feature of the interface calculated here is that it is not monotonic, as the interface between simple fluids must be; that the interface can oscillate is most striking. The elasticity of the chains, and their connectedness, results in this unique effect.

The salient features of this copolymer system are the linear restoring force along each chain (Hooke's law), incompressibility of polymer liquid, and monodispersity along each chain. Incompressibility is easily included in this fluid flow model, and the Hooke's law restoring force is modeled by the quadratic form for the "kinetic" energy density for a small fluid element, as in Eq. (3). Monodispersity can be included as a boundary condition in the first-order problem, or more generally as an integral constraint on the velocity field.

Each of these properties is also manifested in a system composed of an incompressible elastic solid, i.e., rubber. Even under major deformations, rubber is very nearly incompressible. Monodispersity in the rubber system arises naturally. If the material is conceived of as a network of cross-linked chains, monodispersity is equivalent to the microscopic condition that after a deformation is applied, all links are maintained. Elastic forces arise not only in a single direction (along the chain's backbone), but along the cross links too.

In the fluid picture, all transverse forces on a chain arise from the gradient of a scalar pressure field. The exact form of the pressure field is chosen in accord with incompressibility. Transverse forces which do not arise from the gradient of a pressure can arise in the fluid picture when viscosity is included in Eq. (4). The Navier–Stokes equation is thus produced:

$$K \frac{d\mathbf{v}}{dt} = \nabla p + \nu \nabla^2 \mathbf{v}. \quad (128)$$

The question then, is, can the effect of cross linking the chains be captured in Eq. (128)?

The following system of layered rubbers is considered. There is a rubber of type A with the elastic modulus K_A permanently bonded to a rubber of type B with the elastic modulus K_B . This composite is then stretched by a factor λ in the \hat{z} direction. The stress in the rubber is still uniform at

this point, but is no longer isotropic. This situation recalls the zeroth-order lamella, where there are large stresses perpendicular to the AB interface, and none in the plane of the interface. The larger the stretching factor λ , the more the rubber composite approaches the copolymer system.

A small perturbing force is applied at the boundary, by supplying a force at the AB interface which pulls the interface in the \hat{z} direction. This models the difference in wetting forces in the copolymer system. This perturbation results in a small displacement field $\mathbf{u}^{(1)}$. I model the bulk rubber as a collection of masses connected by longitudinal and transverse springs, and let the "at rest" rubber have a constant spacing a between masses. The volume of a cell is thus a^3 . After the initial stretching, the cell occupied by a single mass has the dimensions λa in the z direction, and $a/\sqrt{\lambda}$ in the x and y directions, so the volume occupied by the mass does not change.

With the addition of the small displacement field $\mathbf{u}^{(1)}$, the resultant of the elastic forces gives

$$f_{el} = K a^2 (\lambda^{-1} \partial_{xx} \mathbf{u}^{(1)} + \lambda^2 \partial_{zz} \mathbf{u}^{(1)}). \quad (129)$$

Equilibrium is achieved when this resultant force per unit volume is canceled by whatever pressure gradient is generated:

$$K (\lambda^{-1} \partial_{xx} + \lambda^2 \partial_{zz}) \mathbf{u}^{(1)} = \nabla p. \quad (130)$$

To make a firm connection with the fluid model, the relationship between $\mathbf{u}^{(1)}$ and $\mathbf{v}^{(1)}$ is determined as follows:

$$\mathbf{u}^{(1)} = \int_0^z dz \frac{dn^{(0)}}{dz} \mathbf{v}^{(1)} = \int_0^z dz \frac{\mathbf{v}^{(1)}}{v_0}. \quad (131)$$

Differentiating this equation with respect to z yields

$$\mathbf{v}^{(1)} = \partial_z \mathbf{u}^{(1)} v_0. \quad (132)$$

Thus, in terms of the displacement field, the Navier–Stokes equation reads as follows (when the flow is steady):

$$v_0^2 K \partial_{zz} \mathbf{u}^{(1)} = \nabla p + \nu \nabla^2 \partial_z \mathbf{u}^{(1)}. \quad (133)$$

Thus, the author must make the conclusion that adding viscous forces in the full treatment of the fluid model does not correspond to the physical cross linking of the chains. Comparing Eqs. (130) and (133), it is clear that for any finite value of λ , these equations cannot describe the same physical situation. If the rubber is greatly stretched, so that $\lambda \gg 1$, then Eqs. (130) and (133) are equivalent, only when the viscosity ν is very small.

For λ on of the order of, say 5, the effect of the transverse cross links could be negligible. Typical transverse stresses from the cross links in this case are on the order of $5^3=125$ times smaller than the longitudinal stresses. This value of relative stretching is achievable with currently available copolymers. Thus, an appropriate physical model for the Alexander–deGennes copolymer layer considered here is that of a slightly distorted uniaxially stressed, incompressible, elastic solid.

VIII. CONCLUSION

Young's law for copolymers is derived, that is the shape of the interfacial profile with the lamellar order perpendicular to a flat substrate is determined. This is done by making a model based on familiar ideas from elementary fluid dynamics. The influence of the substrate enters through a parameter $\epsilon = (\gamma_B - \gamma_A)/\gamma$. The shape of the profile is characterized by the wetting angle between A, B, and the substrate, it crosses $z=0$, and recoils, sometimes with an underdamped oscillation, and sometimes with an overdamped oscillation. Only when one of the species of copolymer is completely flexible, $k_A=0$, does this tendency to cross $z=0$ disappear. Near the substrate, the profile contains nonanalytic terms proportional to $x^4 \log x$, a novel property for copolymers. The model presented here exhausts the possible behavior of simple copolymers in this morphology. Finally, the course of this calculation indicates that Alexander-deGennes models, even for large ϵ , can be cast in the familiar language of static fluid flow, for which there is a large body of expertise to draw on.

While the Alexander-deGennes approximation is helpful in making calculations of this sort, it is expected that real copolymers will depart somewhat from the behavior derived here. First, seldom are realistically available copolymers in the strong segregation limit. The chains are not highly stretched, so that the case described here must be extrapolated to from modest molecular weights. Second, as do most current studies of the deformation of a copolymer layer, the author employs the Alexander-deGennes approximation. Thus, the quantitative properties derived here, such as the oscillation wave number, are not exact. And, some of the results, like the weak singularity near the contact line, could be qualitatively different in real copolymer domains.

ACKNOWLEDGMENTS

This research was supported by the US National Science Foundation through its MRSEC Program under Awards Nos. DMR-8819860 and DMR-9400379. The author also benefited from many discussions with Tom Witten and Francisco Solis. This paper has been submitted to the faculty of the Department of Physics at the University of Chicago as a Ph.D. dissertation.

APPENDIX: STIFF MEMBRANE

Here the author describes briefly the form of the interface formed between a simple liquid and air held at a constant pressure, near a hard vertical wall which tends to slightly wet with the fluid. There is a uniform gravitational field. Let $z=0$ be the level of fluid far from the wall. I use this case to compare to the shape of the interface when $k_A=0$. After this, the author generalizes to a system where the interface is characterized by a rigidity as well as a surface energy, and compare this system to the problem with general f and k_A .

When the free surface is given any particular profile, $m(x)$, there are three energies that must be paid. First, there is the interfacial energy associated with making more (or

less) free surface for the fluid. Second, there is the interfacial energy associated with the fluid covering more (or less) of the vertical wall. Finally, there is work that is done by the hydrostatic pressure in the liquid: for small distortions, and for an incompressible liquid,

$$p = p_0 - g\rho m(x), \quad (\text{A1})$$

where p_0 is atmospheric pressure. The difference in pressure across the free surface is

$$\Delta p = g\rho m(x). \quad (\text{A2})$$

Thus, the energy needed to make a small distortion, m , is

$$G[m(x)] = \int_0^\infty 1/2 \left(\gamma \frac{dm}{dx} \frac{dm}{dx} + g\rho m^2 \right) - \gamma_w m(x=0). \quad (\text{A3})$$

Here, γ_w is the interfacial energy to cover a portion of the wall surface with fluid.

Varying this energy with respect to $m(x)$ yields an equation determining $m(x)$:

$$\gamma m'' = g\rho m, \quad (\text{A4})$$

with $x \neq 0$, and the conditions²⁰

$$m(x) \rightarrow 0 \quad \text{as } x \rightarrow \infty, \quad \text{and} \quad (\text{A5})$$

$$m'(x=0) = -\frac{\gamma_w}{\gamma}.$$

The interface is

$$m(x) = \frac{\gamma_w}{\gamma} \lambda e^{-x/\lambda}, \quad (\text{A6})$$

with $\lambda = \gamma g^{-1} \rho^{-1}$. This is exactly the form of the AB interface when $k_A=0$, i.e., when one of the components of the copolymer is completely flexible.

When the interface between the two fluids is characterized by both a surface energy and a bending modulus (e.g., for a surfactant monolayer residing at the air-water interface), the interface closely resembles that of the copolymer system. The presence of a bending modulus results in the oscillation of the interface as per the system described in Ref. 17. It is necessary to add a term to Eq. (A3) describing the energy needed to create curvature locally:

$$G_{\text{bend}} = \int_0^\infty dx \frac{k}{2} \left| \frac{d^2 m}{dx^2} \right|^2, \quad (\text{A7})$$

so that the equation of motion for (small) $m(x)$ is now

$$k \frac{d^4 m}{dx^4} - \gamma \frac{d^2 m}{dx^2} + g\rho m(x) = 0, \quad (\text{A8})$$

with whatever boundary conditions the author later wishes to establish.

Upon Fourier transforming this equation, the solution is given by a linear combination of wave vectors which satisfy

$$kq^4 + \gamma q^2 + g\rho = 0. \quad (\text{A9})$$

When $b \equiv g\rho k / \gamma^2 > 1/4$, the solutions to this equation have both an imaginary (damping) and real (oscillatory) parts.

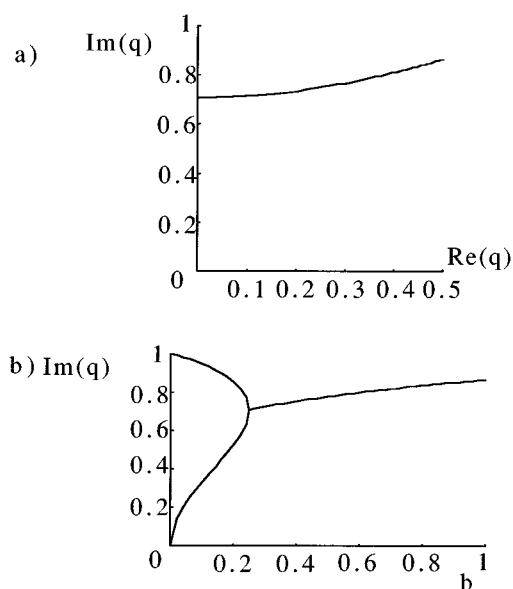


FIG. 7. (a) The solutions of Eq. (A9) are plotted as b is tuned from 1 to 0. (b) The imaginary part of the position of the pole is plotted against b . Notice the similarity to the case with $f=1/2$ with $0 < k_A < 1$ as in Fig. 6.

Figure 7 shows the location of the pole in the first quadrant. Note that as $b \rightarrow \infty$, the oscillations become more and more rapid, and more and more quickly damped. As $b \rightarrow 1/4$ the oscillatory part of the solution disappears, and the solution is made of purely decaying components. This situation closely resembles the case in which k_A is small, and f is decreased from 1 to some intermediate value (at which the oscillatory part of the pole vanishes). Therefore, the AB interface is

characterized by both a rigidity and a surface energy. As a final note, there is no nonanalytic correction to Young's law in this case. Regardless of the type of boundary conditions imposed, the solution is a combination of analytic functions, and is itself analytic.

- ¹F. S. Bates and G. H. Fredrickson, *Annu. Rev. Phys. Chem.* **41**, 525 (1990).
- ²H. Hasegawa and T. Hashimoto, *Polymer* **33**, 475 (1992).
- ³G. T. Pickett, T. A. Witten, and S. R. Nagel, *Macromolecules* **26**, 3194 (1993).
- ⁴T. L. Morkved, P. Wiltzius, H. M. Jaeger, D. G. Grier, and T. A. Witten, *Appl. Phys. Lett.* **64**, 422 (1994).
- ⁵*Nanostructures and Mesoscopic Systems*, edited by W. P. Kirk and M. A. Reed (Academic, New York, 1992).
- ⁶S. Alexander, *J. Phys. (Paris)* **38**, 983 (1977).
- ⁷P.-G. deGennes, *J. Phys. (Paris)* **37**, 1443 (1976); *Macromolecules* **13**, 1069 (1980).
- ⁸S. T. Milner, T. A. Witten, and M. E. Cates, *Europhys. Lett.* **5**, 413 (1988); *Macromolecules* **21**, 2610 (1988).
- ⁹P. deGennes, *Scaling Concepts in Polymer Physics* (Cornell University Press, Ithaca, NY, 1979).
- ¹⁰See, e.g., L. M. Milne-Thompson, *Theoretical Hydrodynamics* (Macmillan, New York, 1955).
- ¹¹P. D. McCormack and L. Crane, *Physical Fluid Dynamics* (Academic, New York, 1973).
- ¹²G. H. Fredrickson, A. Ajdari, L. Leibler, and J.-P. Carton, *Macromolecules* **25**, 2882 (1992).
- ¹³M. S. Turner and J.-F. Joanny, *Macromolecules* **25**, 6681 (1992).
- ¹⁴A. J. Silberberg, *J. Colloid Interface Sci.* **90**, 86 (1982).
- ¹⁵A. N. Semenov, *Zh. Exp. Theor. Phys.* **88**, 1242 (1985), translated in *Sov. Phys. JETP* **61**, 733 (1985).
- ¹⁶J. N. Israelachvili, *Intermolecular and Surface Forces: With Applications to Colloidal and Biological Systems* (Academic, Orlando, 1985).
- ¹⁷N. Dan, P. Pincus, and S. A. Safran, *Langmuir (Lett.)* **9**, 2768 (1993).
- ¹⁸C. Yeung, A. C. Balazs, and D. Jasnow, *Macromolecules* **26**, 1914 (1993).
- ¹⁹F. Solis and G. T. Pickett, *Macromolecules* **28**, 4307 (1995).
- ²⁰A. W. Adamson, *Physical Chemistry of Surfaces* (Wiley, New York, 1990).